Available online at www.sciencedirect.com

ScienceDirect

Procedia CIRP 61 (2017) 588 – 593

www.elsevier.com/locate/procedia

The 24th CIRP Conference on Life Cycle Engineering

Dynamical fatigue behavior of additive manufactured products for a fundamental life cycle approach

Eckart Uhlmann[a], Claudia Fleck[b], Georg Gerlitzky[a*], Fabian Faltin[a]

[a]*Institut für Werkzeugmaschinen und Fabrikbetrieb (IWF), TU Berlin, Pascalstraße 8-9, Berlin 10587, Germany*
[b]*Institut für Werkstoffwissenschaften und-technologien TU Berlin, Straße des 17. Juni 135 10623, Germany*

* Corresponding author. Tel.: +49-30-314-24962; fax: 49-30-314-24962. *E-mail address:* gerlitzky@iwf.tu-berlin.de

Abstract

Additive Manufacturing (AM) processes are increasingly integrated into today's value added chains and are prospectively used for batch production. Due to the fact that conventional manufacturing technologies feature design and machining restrictions AM processes offer a nearly restriction free design freedom. This fact could be an answer to the permanent increase in demands of today's products. However, additive manufactured parts suffer from bad surface quality and the material properties concerning fatigue life are still an objective of current investigations. As a first step to describe the Life Cycle of additive manufactured parts fundamental knowledge about the dynamical fatigue behavior in operation has to be obtained. In comparison to conventional machined products this knowledge is not available to this extent for additive manufactured products. It is crucial to ensure that AM parts have a comparable or better high cycle fatigue (HCF) behavior compared to conventional machined parts for the potential future use as dynamical loaded parts in the aviation industry and medical technology such as turbine blades or implants. We investigate additive manufactured parts concerning the HCF behavior and surface quality. The parts are machined with Selective Laser Melting and then investigated concerning surface roughness and fatigue life. Also different finishing processes after the AM process are investigated in order to find out how different process chains influence the HCF behavior of additive manufactured parts.

Peer-review under responsibility of the scientific committee of the 24th CIRP Conference on Life Cycle Engineering

Keywords: Additive Manufacturing; Selective laser melting; Fatigue life

1. Introduction

Compared to conventional manufacturing processes Selective Laser Melting (SLM) is a very young manufacturing process. However its relevance is steadily growing in production, as it empowers the fast production of prototypes and serial components. This is due to the advantage to manufacture components with nearly no geometrical restrictions. Therefore, Selective Laser Melting delivers an answer to the continuously increasing complexity of serial components and enables the resource saving manufacturing of complex parts and hard to machine components [1]. Especially in the aviation industry SLM and Additive Manufacturing is already successfully adapted for serial components due to the expensive materials used and the high material removal of conventional manufacturing processes. Additive manufacturing applications compared to conventional manufacturing process are only sustainable and cost efficient on certain business cases. According to [6], [7] additive manufacturing should be preferred at low production volumes, high material cost and high machining costs while conventional manufacturing processes should be used at large production volumes, low material costs and easy to machine materials. This is mainly due to the fact that the fixed costs of the additive manufacturing process are lower than the fixed costs of comparable conventional manufacturing processes while the recurring costs of additive manufacturing processes are 1.5-2 times higher than conventional manufacturing

Peer-review under responsibility of the scientific committee of the 24th CIRP Conference on Life Cycle Engineering
doi:10.1016/j.procir.2016.11.138

processes [6]. Due to these facts it is clearly visible that the business case drives the application and it should be carefully examined whether a product is manufactured with AM. Other aspects of sustainability which favor AM compared to conventional manufacturing processes are less waste generation, ability to create on demand spare parts which reduces inventories or the ability to produce optimized geometries with near perfect weight to strength ratios which results in a lower carbon footprint and less embodied energy of the product [8]. Currently the main problems concerning Additive Manufacturing processes are the achievable surface quality, geometrical accuracy, uncertainty about mechanical properties and high costs [2]. Due to these problems SLM manufactured parts often need to be finished by a post process. In this paper the dynamical fatigue behavior of selective melted parts are investigated. Because of the common use of a post process, the parts are finished with two different processes, turning and vibratory finishing and then the fatigue life of the differently finished parts is compared to the fatigue life of the not finished parts.

2. Selective Laser Melting

Selective Laser Melting is a layer Additive Manufacturing process for metallic materials. The process is used to manufacture prototypes, tools and serial components out of metallic powder with a steady growing market and applications [3]. The basic concept of all Additive Manufacturing processes is identical; the geometrical information is delivered by a 3D CAD model which is then sliced into layers of a defined layer thickness. The Additive Manufacturing process is then divided into 2 steps, powder deposition and exposing which are constantly repeated, illustrated in fig 1.

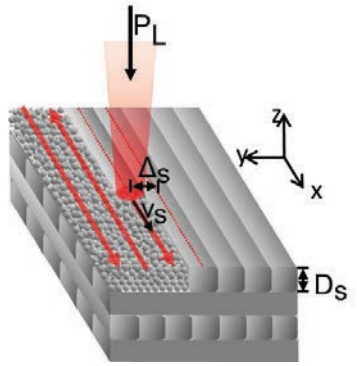

Figure 1Schematic illustration of the SLM process

A laser beam and scanning system are used to expose the part and bind the powder while a scrapper or roller deposits the powder. The main advantages of this process are the geometrical freedom of the produced parts and the possibility to realize inner contours. However, additive manufactured parts suffer from bad surface quality and the lack of fundamental knowledge about their fatigue behavior. This hinders the possible applications for additive manufactured parts in dynamically loaded operations.

3. Experimental Setup

All parts were produced on the SLM machine SLM 250 HL, MTT Technologies GmbH, Lübeck, located at the Production Technology Center in Berlin, Germany. An overview of the machine specifications are given in table 1.

Table 1 Machine specifications

Building space	250mm*250mm*350mm
Max. Laser Power $P_{L,max}$	400W
Layer thickness D_S	20..100µm
Focal point diameter d_f	70..300µm
Building speed v_b	5..20cm³/h

3.1. Powder characterization and built parameters

To produce the parts stainless steel powder 316L (1.4404) was used with a grain size distribution of 20 to 63µm. The powder properties were obtained from the suppliers' certificate following European standard DIN EN 10204.
The parts were produced with optimized building parameters regarding density of the part and are shown in table 2.

Table 2 Building parameters

Layer thickness D_S	0,05mm
Laser power P_L	275W
Scanning speed v_S	760mm/s
Hatch pattern	chess
Hatch distance Δ_S	0,12mm

3.2. Test specimen

Two different specimen geometries were produced depending on the different post processes (figure 2)

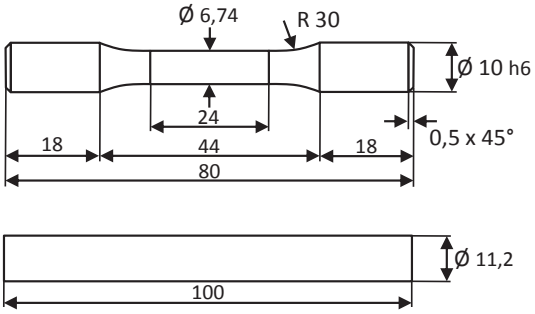

Figure 2 Dimensions of different specimen

Figure 3 Different specimens after production

Specimen A was produced with SLM and post processed with turning which lead to specimen D (figure 3). Specimen B was produced with SLM with no further post process. Specimen C was produced with SLM followed by an additional vibratory finishing process. The parameters for the turning and the vibratory finishing process are given in table 3.

Table 3 Overview of finishing process parameters

Turning process		
Depth of cut a_e	0.5mm	
Feed f	0.15mm/U	
Cutting speed v_c	140m/min	
Vibratory finishing process	1st process step	2nd process step
Processing time t_p	120min	60min
Abrasive media	Triangular	Cylindrical
Excitation frequency f_E	50Hz	50Hz

The turning process was carried out on a CTX gamma 1250 CT machine from DMG Mori Europe Holding AG, Winterthur. The vibratory finishing process was carried out as a two stage process on a MF 8/1, Multi finish GmbH & Co. KG, Schömberg. In a first process step triangular abrasive media was used for a process time of 120 minutes. In a second process step cylindrical abrasive media was used for a process time of 60 minutes.

4. Experimental procedure and results

Initially 60 specimens were produced with SLM followed by the different post processes turning and vibratory finishing. In total 20 of each kind of specimens (B, C and D) were produced. Subsequently, for all specimens the surface roughness was determined. After this, all specimens were tested regarding their high cycle fatigue behavior on the Punz machine. The microstructure and the fracture behavior of one typical specimen of each kind was investigated by light and scanning electron microscopy (LM, SEM), respectively.

4.1. Microstructural investigations

For the microstructural characterization, longitudinal and cross-sections of each kind of specimen were prepared. The longitudinal sections contain the area of the fracture origin and the final fracture, the cross-sections are situated about 1 cm below the fracture surface. After grinding and polishing, the sections were etched with V2A-etchant to develop the microstructure.

Figure 4 shows the typical microstructure of the SLM manufactured specimens. The cross-sections nicely represent the hatch pattern of the manufacturing process. Each of the longitudinal structures is made up of many grains which lack the polygonal structure usually observed in austenitic steels. In some areas, dendrites are visible. All specimens contain binding defects, visible as black voids. The surface of the turned specimen is smooth with some voids present. The longitudinal section (fig. 4a2) further shows a secondary crack that runs through a binding defect just below the surface. We may assume that this fatigue crack originated at this defect but could not develop into a dominant crack due to higher crack growth in the level of the later fracture surface. The surface of the vibratory finished specimen is also very smooth, and the microstructure just below the surface looks plastically deformed. Nevertheless, more shallow defects are visible on the surface than on the turned surface. The SLM shape specimen has a very rough surface. Numerous large defects and molten and re-solidified powder particles are visible.

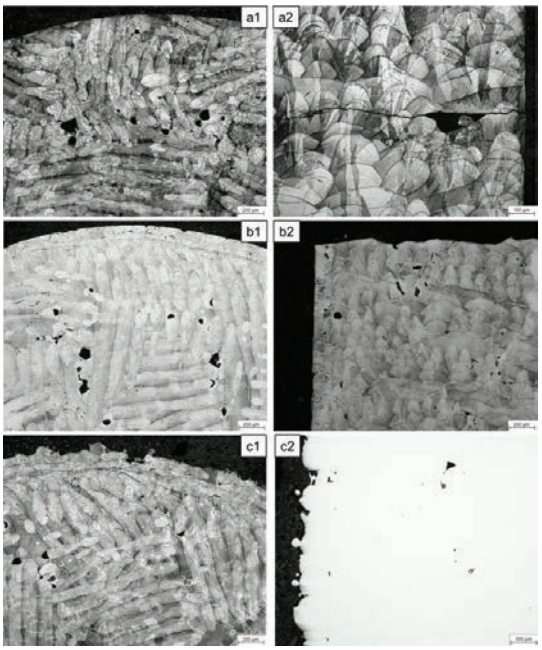

Figure 4 LM: cross-sections (left row, “1”) and longitudinal sections (right row, “2”) of a) turned, b) vibratory finishing, c) slm shape specimens. Note the different scale of b2 as compared to a2 and c2.

4.2. Roughness measurements

All surface roughness measurements were conducted with the tactile measurement system Hommel Nanoscan etamic 855, Jenoptik, Jena. The investigated target values were Ra and Rz. All specimens were measured three times and turned by 120 degrees to ensure reproducibility for all measurements. The average value of these three measurements was taken to obtain the target value of one specimen. In addition, the mean standard deviation was calculated for all measurements.

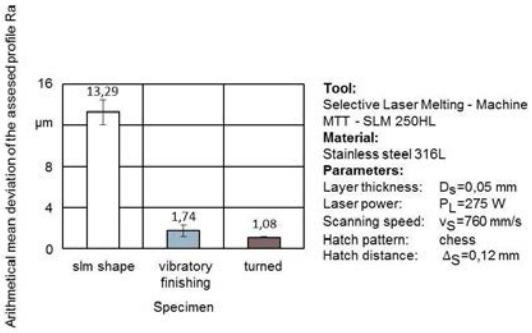

Figure 5 Arithmetical mean deviation of the assessed profile Ra

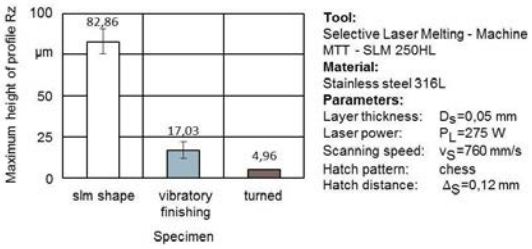

Figure 6 Maximum height of profile Rz

Figure 5 and 6 show the measured target values Ra and Rz for the different specimens. The SLM shape specimens have by far the highest surface roughness of all specimens with a roughness Ra of 13.29 and Rz of 82.86. The vibratory finished specimens have a mean arithmetic surface roughness Ra of 1.74 and Rz of 17.03. Turned specimens showed the best surface roughness with Ra of 1.08 and Rz 4.96. The vibratory finished specimens have a significantly higher surface roughness than the turned specimen for both target values Ra and Rz. Better surface qualities for the vibratory finishing process could be obtained with a longer process time and special abrasive media, due to the fact that fatigue resistance is highly dependent on the surface roughness [4]. This may lead to a low fatigue resistance of the SLM shaped specimen, with the turned specimen possibly showing the best fatigue resistance. The measurements also revealed the highest standard deviation for SLM shape specimen. The high surface roughness is mainly due to the fact that the typical particle size distribution for the SLM process is 20 to 63µm. This limits the achievable surface quality. With a smaller particle size distribution better surface qualities would be achievable but this contains other risks and problems such as respirability of the finer powder and worse flowabilty of the powder. The higher standard deviation has two possible reasons. First, the poor reproducibility of SLM manufactured parts, this is due to different temperatures in the melt pool which are caused by a non-symmetrical protective gas flow and the location of the part during the process which causes different heat transfer coefficients. The second reason is the measurement systems. Due to the high surface roughness optical as well as tactile measurement systems reach their limits [5]. Optical measurement systems struggle with reflecting surfaces while the stylus tip of a tactile measurement can break due to possible undercuts and pores of the selective laser melted part.

4.3. High cycle fatigue (HCF) test series

High cycle fatigue tests were performed with a rotating bending machine (Carl Schenck AG, Darmstadt, type Rapid *Punz*) at a frequency of 100 Hz under air cooling to a maximum number of cycles (N_{max}) of 10^7. Two surface stress amplitudes were chosen in the HCF range for each finishing state to yield numbers of cycles to failure (N_f) of about $5 \cdot 10^5$ and $2 \cdot 10^6$. Further specimens were tested at lower surface stress amplitudes, in the transition range to the endurance limit.

Figure 7 shows the results of the rotating bending tests. The dashed lines in the HCF regime are a guide for the eye to highlight the fatigue life ranges of the differently finished SLM specimens. The gray arrows denote specimens that did not fail at cycle numbers above the defined maximum number of cycles to failure (N_{max}, denoted by the bold black line). The SLM shape specimens exhibit the lowest fatigue life resistance. After vibratory finishing or turning, the life expectancy increases clearly. The differences seem to be slightly higher for higher surface stress amplitudes, and slightly lower for stress amplitudes in the transition range. The SLM shape and vibratory finished specimens show a huge scatter in the fatigue life, specifically in the transition range, with specimens failing at around $2 \cdot 10^6$ while others survive $2 \cdot 10^7$ cycles at the same surface stress amplitude. For the turned specimen, the numbers of cycles to failure scatter much less in this fatigue range. The results of the fatigue tests correlate well with the differences in surface roughness between the specimen types. Local height variations on the surface originating from the powder particle size, as in the SLM shape specimens, or from turning marks as in the turned specimens, act as stress raisers. Fatigue failures usually originate from the surface; furthermore, in rotating bending tests the highest tensile stresses act at the surface. Rougher surface states result in locally even higher stresses, corresponding with lower numbers of cycles to failure. The higher fatigue endurance of the vibratory finished and turned specimens may further be due to compressive residual stresses originating from the finishing procedures. Further, defects just below the surface might be compressed by plastic deformation near the surface.

4.4. SEM analysis

The fracture surfaces of selected specimens, all tested with surface stress amplitudes leading to failure within 106 cycles, were investigated by scanning electron microscopy (SEM; CamScan REM Serie 2, Obducat, Lund, Sweden) at an accelerating voltage of 20 kV in the secondary electron mode. The specimens were cut about 1 cm below one of the fracture surfaces under continuous water-cooling while the fracture surfaces were protected by a polymer cover, and imaging was performed after ultrasonic cleaning in ethanol.

Typical fracture surfaces of specimens that failed at about 10^6 cycles are shown in figure 8. The surveys in the upper row show the smoother fatigue and rough final fracture areas. All specimens exhibit several failure origins, denoted by arrows: the continuous arrows with a bold head point to the one (a1, b1) or two (c1) main, dominant fracture origin(s), and the dashed arrows with a line-head point to additional non-dominant origins. The higher magnification micrographs in the bottom row show the area of the dominant, or of one of the dominant fatigue origins on the fracture surfaces together with the specimen surfaces nearby. All fatigue failure(s) originated at binding defects at (a2, b2) or just below (c2) the surface. Please note that the magnified sections of the vibratory finished and the turned specimen are oriented in the same direction as the survey above while the SLM shape specimen has been rotated clock-wise by 90° to acquire the magnified view.

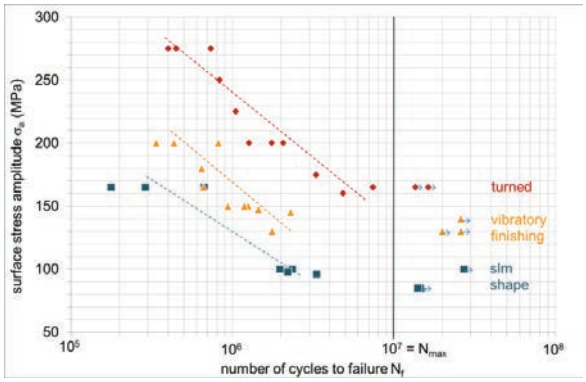

Figure 7 S,N-curves for SLM-316L specimens

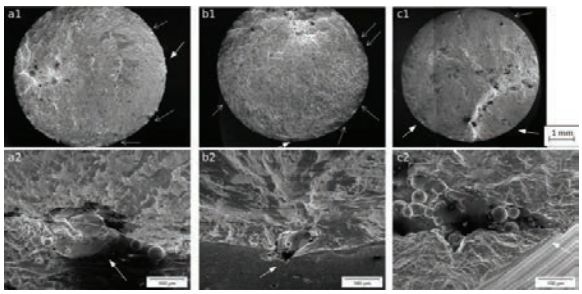

Figure 8 SEM micrographs of fracture surfaces of specimens with different surface finishing: a) turned, b) vibratory finishing, c) SLM shape; all loaded with surface stress amplitudes leading to numbers of cycles to failure in the range of $N_f = 10^6$:

While the SLM shape specimens exhibit a rough surface, with rounded powder particles clearly visible (a2; the white dashed line serves as a guide to the eye to discriminate the fracture and specimen surfaces above and below the line, respectively), the vibratory finished specimens have a relatively even and smooth surface (b2). Turning marks are visible on the surfaces of the turned specimens (c2). Inner defects just below the surface act as local stress raisers; together with the different surface roughness features and possible compressive residual stresses in the surface finished states, they define the local stress state, and failure starts where the local tensile stresses are highest (comp. figure 4a2).

The final fracture surfaces show dimples, as to be expected for the inherently ductile austenitic materials, and occasional fatigue striations were observed on the fatigue fracture surfaces (data not shown). The black areas on the micrographs are due to charging effects of only partially attached or less electron-conductive particles on the surfaces and fracture surfaces, usually found within depressions.

4.5 Comparison with state of the art fatigue testing

Fatigue testing of additive manufactured products has already been investigated by some researchers e.g. [9], [10], [11]. The main testing method was the four point bending test as in this work. Often the main focus was to compare different heat treatment strategies or build orientations to ensure the best possible fatigue life [10], [11]. In some works even a concrete product was produced with AM and successfully dimensioned in terms of fatigue life [9]. The results in this work correlate well with other works regarding the dependency of roughness and fatigue life. A unique feature of this work is to reveal the differences between the examined process chains regarding fatigue life as well as different fracture behaviors. This should be helpful to identify a reasonable holistic process chain for AM.

5. Conclusion and outlook

In this work we investigated the influence of three different finishing methods for SLM manufactured specimens regarding their fatigue behavior. The investigated material was stainless steel 316L. The fundamental approach showed that the bad surface quality of additive manufactured parts is a key problem of this technology, not only for functional surfaces, but as well for the fatigue life. Turned specimens showed the best fatigue behavior while SLM manufactured specimens showed the worst. This correlates well with the obtained surface roughness, also the data for fatigue life of SLM manufactured and vibratory finished specimens scatter a lot. These results demonstrate the importance of integrating the SLM process into an appropriate and cost efficient process chain to increase the fatigue life of additive manufactured parts and spread the applications possibilities of Selective Laser Melting. In the future other hard to machine materials, produced by SLM, such as titanium or Inconel which are used for dynamically loaded operations in aviation should be investigated. In addition the conventional process chain should be compared with the additive manufacturing process

chain regarding fatigue life of the produced parts. In terms of life cycle thinking a process chain should be developed which still features the sustainable aspects of AM linked with a better surface roughness and fatigue life.

Acknowledgements

CF thanks Dr. R. Meinke for support with the rotating bending tests and for performing the SEM microscopy, M. Schaube and M. Richter for the metallographical preparation and R. Engelmayer for technical support.

References

[1] Meiners, W. Direktes Selektives Laser Sintern einkomponentiger metallischer Werkstoffe, Dissertation, Shaker Verlag, Aachen, 1999.
[2] E. Yasa, J-P. Kruth, J. Deckers. Manufacturing by combining Selective Laser Melting and Selective Laser Erosion/laser re-melting. CIRP Annals-Manufacturing Technology, 263-266, 2011.
[3] Wohlers, T. Wohlers report: Additive manufacturing and 3D printing state of the industry.
[4] E. Uhlmann, P. John, V. Kashevko, G. Gerlitzky, A. Bergmann. Quality optimized Additive Manufacturing through Measuring System Analysis. Proceedings, ASPE Spring topical meeting, 83-88, 2015.
[5] M. Suraratchai, J. Limido, C. Mabru, R. Chieragatti. Modelling the influence of machined surface roughness on the fatigue life of aluminium alloy. International Journal of fatigue, Vol 30, 12, 2119-2126.
[6] W. Frazier. Metal Additive Manufacturing: A review. Journal of Materials Engineering and performance, Vol 23 ,6, 1917-1928, 2014.
[7] S.Ford, M. Despeisse. Additive manufacturing and sustainability: an exploratory study of the advantages and challenges. Journal of cleaner prduction Vol 137, 1573-1587, 2016.
[8] M. Mani, K. E. Lyons, S. K. Gupta. Sustainability characterization for additive manufacturing. Journal of Research of the National Institute of Standards and Technology, Vol 119, 419-428, 2014.
[9] Stoffregen, H., Butterweck, K., Abele, E., Fatigue analysis in selective laser melting: Review and investigation of thin- walled actuator housings, 25th Solid Freeform fabrication symposium, Austin, Texas, 2014.
[10] Spierings, A. B., Starr, T. L., Wegener, K. Fatigue performance of additive manufactured metallic parts, Rapid Prototyping Journal, Vol 19 (2), 88-94, 2013.
[11] Sehrt, J.T. Witt, G. Dynamic strength and fracture toughness analysis of beam melted parts. Proceedings of the 36th International MATADOR cpnference, 385-388, 2010.